INDERSCIENCE PUBLISHERS
Linking academia, business and industry through research

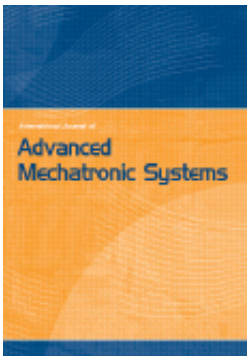

International Journal of Advanced Mechatronic Systems

ISSN online: 1756-8420 - ISSN print: 1756-8412
https://www.inderscience.com/ijamechs

Model-free design in a dual-rate system using finite impulse response filter

Takao Sato, Natsuki Kawaguchi

DOI: 10.1504/IJAMECHS.2024.10063119

Article History:

Received:	29 June 2023
Last revised:	30 July 2023
Accepted:	20 September 2023
Published online:	25 March 2024

Model-free design in a dual-rate system using finite impulse response filter

Takao Sato* and Natsuki Kawaguchi

Graduate School of Engineering,
University of Hyogo,
2167 Shosha, Himeji,
Hyogo 671-2280, Japan
Email: tsato@eng.u-hyogo.ac.jp
Email: kawagouchi@eng.u-hyogo.ac.jp
*Corresponding author

Abstract: In model matching design, the controller is determined by minimising the matching error between the reference model and the actual control system. Virtual reference feedback tuning (VRFT), a data-driven approach, uses a pre-filter to compensate for matching errors between model-based and data-driven functions. Designing the pre-filter in the time domain rather than the frequency domain allows the controller to be designed without limiting the types of initial process inputs. Conventional time-domain-based VRFT is designed as a single-rate method that is uniform over the entire period. When certain periods are limited by hardware performance or other factors, performance can be improved by setting the unrestricted period independently of the restricted period. In this study, time-domain-based VRFT is extended to a dual-rate system where the sampling period of the process output and the holding period of the process input are different. The control performance of the proposed dual-rate system is superior to that of the conventional single-rate system because the process input can be updated more frequently than in the single-rate system, even when the sampling period is limited by sensor performance or computational load.

Keywords: model free; finite impulse response; FIR; holding period; sampling period.

Reference to this paper should be made as follows: Sato, T. and Kawaguchi, N. (2024) 'Model-free design in a dual-rate system using finite impulse response filter', *Int. J. Advanced Mechatronic Systems*, Vol. 11, No. 1, pp.1–10.

Biographical notes: Takao Sato is a Professor at the University of Hyogo, Himeji, Hyogo, Japan. He received his PhD from the Okayama University, Okayama, Japan, in 2002. Since 1999, his primary research has been in adaptive control, multi-rate system, autonomous decentralised system, and biological system control.

Natsuki Kawaguchi received his DEng from the University of Hyogo in 2018. He is an Assistant Professor in the Graduate School of Engineering at the University of Hyogo. His research interests are fault detection and fault tolerant control.

This paper is a revised and expanded version of a paper entitled 'Dual-rate data-driven design in the time domain' presented at 2022 International Conference on Advanced Mechatronic Systems, Toyama, Japan, 19 December 2022.

1 Introduction

Society 5.0 (Fukuyama, 2018) is proposed in the Fifth Science and Technology Basic Plan as the future society that Japan should aspire to, and will be realised through a system that highly integrates cyberspace and physical space. In Society 5.0, the internet of things (IoT) and artificial intelligence (AI) will collect, analyse, and determine necessary information, and incorporate advanced technologies into all industries and social life, thereby achieving both economic development and solving social issues.

In this new society, data itself is becoming increasingly important. The importance of data has been reaffirmed in the field of control engineering as well, and data-driven methodologies, which design control systems directly from data, are attracting attention (Prag et al., 2022). Data-driven design methodologies are mainly divided into iterative and non-iterative approaches. In the iterative approach (Hjalmarsson et al., 1998; Bruyne, 2003; Yokoyama et al., 2015; Yokoyama and Masuda, 2016), the optimal solution is obtained through repeated control trials and optimisation, while in the non-iterative approach (Yahagi and Kajiwara, 2022), the optimal solution is obtained based on one-shot control data. Both approaches have their advantages and

disadvantages, while this study focuses on the advantage of obtaining the optimal solution from one-shot trials and discusses design methods in the time domain in the non-iterative approach.

Various non-iterative methods have been proposed, including robust design (Rojas and Vilanova, 2012; Bertsimas et al., 2018) and model matching problems (Breschi et al., 2021; Breschi and Formentin, 2021). Data-driven methods for single-rate systems, such as virtual reference feedback tuning (VRFT) (Campi et al., 2002; Gonçalves da Silva et al., 2016), fictitious reference iterative tuning (FRIT) (Kaneko et al., 2012), and non-iterative correlation-based tuning (NCbT) (Yubai et al., 2011), have since been extended to dual-rate systems (Ito et al., 2018b,a; Sato et al., 2021b,a, 2022). In sampled data control systems (Chen and Francis, 1995), where a continuous-time process is controlled by a discrete-time controller, dual-rate systems that allow multiple signal periods can be designed to be more flexible than single-rate systems (Sato et al., 2013).

Since most conventional dual-rate data driving methods design controllers based on the model matching problem, it is important to design a pre-filter that compensates for the matching error between the original objective function and the actual objective function. Matsui et al. have proposed a pre-filter design method in the time domain (Matsui et al., 2016, 2017). In such time-domain design, the controller can be designed without limiting the input signals. However, conventional time-domain designs have been proposed for single-rate systems. Since the performance of dual-rate systems is expected to be better than that of single-rate systems, this study extends data-driven time-domain design to dual-rate systems. The effectiveness of the proposed method is verified by numerical examples.

The remainder of this paper is organised as follows. In Section 2 a process controlled as a dual-rate system and the control law for controlling it are described, and the design method of the control law is shown in Section 3. Section 4 shows the effectiveness of the proposed method through numerical examples, and Section 5 concludes this study.

Herein, I_i denotes an $i \times i$ identity matrix, and $\otimes$ denotes the Kronecker product.

2 System description

A controlled process is a linear time-invariant continuous-time single-input-single-output (SISO) system, and it is controlled using digital processors operated in discrete time domain. There are hence the sampling periods of continuous-time signals and the holding periods of discrete-time signals. The process dynamics are given as follows:

$$\psi(z) = G(z)\upsilon(z) \tag{1}$$

where $\psi(z)$ and $\upsilon(z)$ are the Z-transforms of process output $\psi(k)$ and input $\upsilon(k)$, respectively and $G(z)$ denotes a process model and is assumed to be unknown. In this study, the process is controlled in a dual-rate system as shown in Figure 1(a), the sampling period of a process output, T_s, is an integer (m) multiple of the holding period of a process output, T_h, and the dual-rate process model is expressed as follows:

$$\begin{aligned}\psi(z) &= \boldsymbol{G}(z)\boldsymbol{\upsilon}(z)\\ \boldsymbol{\upsilon}(z) &= [z^{-m+1}\upsilon(z)\ z^{-m+2}\upsilon(z)\ \dots\ \upsilon(z)]^\top\end{aligned} \tag{2}$$

$\boldsymbol{G}(z)$ is the lifted system of $G(z)$ and is also unknown. In this study, a control law is designed based on data.

Consider the feedback control system illustrated shown in Figure 1(b), where the process is controlled using a fixed-structure control law as follows:

$$\boldsymbol{\upsilon}(z) = \boldsymbol{\Gamma}(z,\boldsymbol{\vartheta})\epsilon(z) \tag{3}$$

$$\boldsymbol{\Gamma}(z,\boldsymbol{\vartheta}) = \boldsymbol{D}(z)\boldsymbol{\vartheta} \tag{4}$$

$$\epsilon(z) = \psi_r(z) - \psi(z) \tag{5}$$

where $\boldsymbol{D}(z)$ and $\boldsymbol{\vartheta}$ are the controller structure and controller parameters, respectively, and $\psi_r(z)$ is the Z-transform of a reference input $\psi_r(k)$. Based on collected control data, $\boldsymbol{\vartheta}$ is determined based on a model matching error.

Figure 1 Dual-rate system, (a) output and input periods (b) block diagram

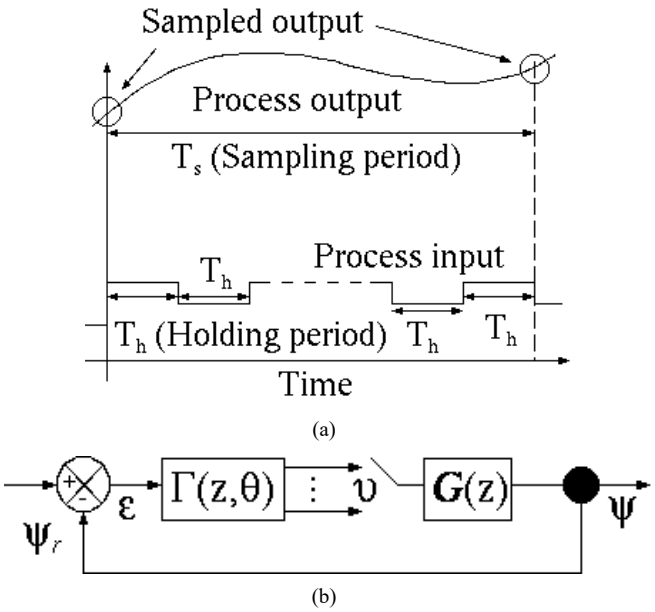

Notes: T_s: output period, T_h: input period.

3 Data-driven design in dual-rate system

The design objective is to match a closed-loop system to a reference model, and the objective function is defined as follows:

$$J_0(\boldsymbol{\vartheta}) = \|\epsilon_0(z,\boldsymbol{\vartheta})\|_2^2 \tag{6}$$

$$\epsilon_0(z,\boldsymbol{\vartheta}) = F_W(z)\left(\Omega(z) - G_{cl}(z)\right) \tag{7}$$

$$G_{cl}(z) = \frac{\boldsymbol{G}(z)\boldsymbol{\Gamma}(z,\boldsymbol{\vartheta})}{1 + \boldsymbol{G}(z)\boldsymbol{\Gamma}(z,\boldsymbol{\vartheta})} \tag{8}$$

where $G_{cl}(z)$ is the closed-loop system from the reference input to the process output, $\Omega(z)$ is the reference model that $G_{cl}(z)$ should match, and $F_W(z)$ is a weighting factor.

In contrast to a dual-rate system, a single-rate system in which the holding period must equal the sampling period is designed as shown in Figure 2, and its objective function is given as follows:

$$J_0^{SR}(\boldsymbol{\vartheta}) = \left\|\epsilon_0^{SR}(z,\boldsymbol{\vartheta})\right\|_2^2 \tag{9}$$

$$\epsilon_0^{SR}(z,\boldsymbol{\vartheta}) = F_W^{SR}(z)\left(\Omega(z) - G_{cl}^{SR}(z)\right) \tag{10}$$

$$G_{cl}^{SR}(z) = \frac{G(z)\Gamma(z,\boldsymbol{\vartheta})}{1+G(z)\Gamma(z,\boldsymbol{\vartheta})} \tag{11}$$

where $\Gamma(z,\boldsymbol{\vartheta})$ is a single-rate control law. When the sampling period is the same for the dual-rate single-rate systems, the process input in the dual-rate system can be updated more frequently than in the single-rate system. Therefore, the control performance of the dual-rate system can be improved over that of the single-rate system.

Figure 2 Single-rate system, (a) output and input periods (b) block diagram ($T_s = T_h$)

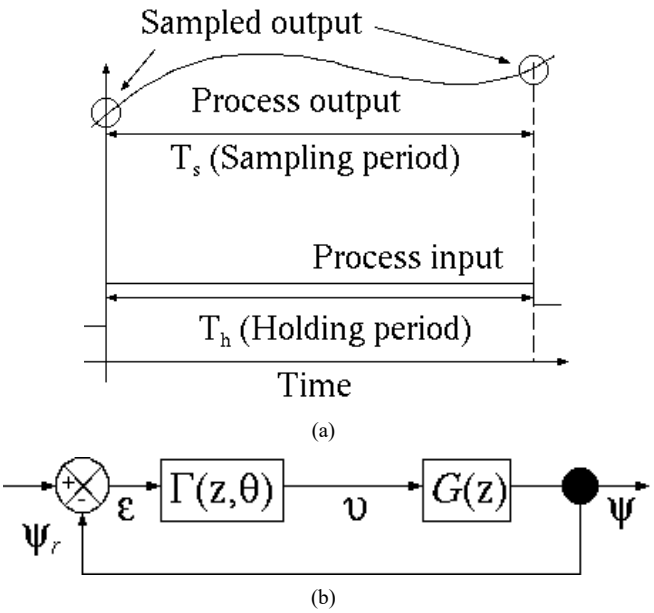

In the objective function equation (6), process model $\boldsymbol{G}(z)$ is included, and the function cannot be directly minimised when the model is unknown. In this study, the next lemma is introduced.

Lemma 1: Equation (12) is equal to equation (6).

$$J(\boldsymbol{\vartheta}) = \|\epsilon(z,\boldsymbol{\vartheta})\|_2^2 \tag{12}$$

$$\epsilon(z,\boldsymbol{\vartheta}) = \boldsymbol{F_L}(z)[\boldsymbol{\upsilon}_0(z) - \boldsymbol{\Gamma}(z,\boldsymbol{\vartheta})\bar{\epsilon}(z)] \tag{13}$$

$$\bar{\epsilon}(z) = \bar{\psi_r}(z) - \psi_0(z) \tag{14}$$

$$\bar{\psi_r}(z) = \frac{1}{\Omega(z)}\psi_0(z) \tag{15}$$

$$\boldsymbol{F_L}(z) = F_W(z)(1-\Omega(z))\Omega(z)\boldsymbol{\Upsilon}_0^{-1}(z), \tag{16}$$

where $\boldsymbol{\upsilon}_0(z)$ and $\psi_0(z)$ are initial control input/output data that are measured from open-loop or closed-loop control. An inverse filter $\boldsymbol{\Upsilon}_0^{-1}(z)$ outputs a unit impulse function when $\upsilon_0(k)$ is input, and the relationship in the Z domain is described as follows:

$$\boldsymbol{\Upsilon}_0^{-1}(z)\boldsymbol{\upsilon}_0(z) = 1. \tag{17}$$

$\boldsymbol{\Upsilon}_0^{-1}(z)$ is designed in the time domain as a finite impulse response (FIR) filter:

$$\boldsymbol{\Upsilon}_0^{-1}(z) = \boldsymbol{\nu}_0^\top + \boldsymbol{\nu}_1^\top z^{-1} + \ldots + \boldsymbol{\nu}_{N_\upsilon-1}^\top z^{-(N_\upsilon-1)} \tag{18}$$

where N_υ is the design parameter and is assumed to be sufficient large to satisfy equation (17). The determination of the coefficients in equation (18) is given in Appendix.

In contrast to the proposed method, which is designed in the time domain, in the conventional dual-rate data-driven method (Sato et al., 2021b), $\boldsymbol{F_L}(z)$ is designed instead of equation (16) as the lifted vector of $F_L(z)$ which is designed in the frequency domain as follows:

$$\begin{aligned}&|F_L(e^{j\omega})|^2\\ &= |F_W(e^{j\omega})|^2|1-\Omega(e^{j\omega})|^2|\Omega(e^{j\omega})|\frac{1}{\Phi_\upsilon}\\ &\forall\omega\in[-\pi;\pi],\end{aligned} \tag{19}$$

where Φ_υ is the spectral density of $\upsilon(k)$.

Proof: First, assume the following equation:

$$\Omega(z) = \frac{\boldsymbol{G}(z)\boldsymbol{\Gamma}^*(z)}{1+\boldsymbol{G}(z)\boldsymbol{\Gamma}^*(z)}, \tag{20}$$

where $\boldsymbol{\Gamma}^*(z)$ is an ideal controller, and the equation is transformed as follows:

$$1-\Omega(z) = \frac{1}{1+\boldsymbol{G}(z)\boldsymbol{\Gamma}^*(z)}. \tag{21}$$

Using equation (20), equation (7) is rewritten as follows:

$$\begin{aligned}&\epsilon_0(z,\boldsymbol{\vartheta})\\ &= F_W(z)\frac{\boldsymbol{G}(z)(\boldsymbol{\Gamma}^*(z)-\boldsymbol{\Gamma}(z,\boldsymbol{\vartheta}))}{(1+\boldsymbol{G}(z)\boldsymbol{\Gamma}^*(z))(1+\boldsymbol{G}(z)\boldsymbol{\Gamma}(z,\boldsymbol{\vartheta}))}\end{aligned} \tag{22}$$

Using equations (20) and (21), equation (13) is also rewritten as follows:

$$\epsilon(z,\boldsymbol{\vartheta}) = \boldsymbol{F_L}(z)[\boldsymbol{\upsilon}_0(z) - \boldsymbol{\Gamma}(z,\boldsymbol{\vartheta})\frac{1}{\boldsymbol{G}(z)\boldsymbol{\Gamma}^*(z)}\psi_0(z)]. \tag{23}$$

From equation (2), $\psi_0(z) = \boldsymbol{G}(z)\boldsymbol{\upsilon}_0(z)$, and equation (23) is rewritten as follows:

$$\epsilon(z,\boldsymbol{\vartheta}) = \frac{\boldsymbol{G}(z)(\boldsymbol{\Gamma}^*(z)-\boldsymbol{\Gamma}(z,\boldsymbol{\vartheta}))}{\boldsymbol{G}(z)\boldsymbol{\Gamma}^*(z)}\boldsymbol{F_L}(z)\boldsymbol{\upsilon}_0(z). \tag{24}$$

In order to make equation (22) equal to equation (24), the following equation must be satisfied:

$$\begin{aligned}&\frac{1}{\boldsymbol{G}(z)\boldsymbol{\Gamma}^*(z)}\boldsymbol{F_L}(z)\boldsymbol{\upsilon}_0(z)\\ &= F_W(z)\frac{1}{(1+\boldsymbol{G}(z)\boldsymbol{\Gamma}^*(z))(1+\boldsymbol{G}(z)\boldsymbol{\Gamma}(z,\boldsymbol{\vartheta}))}.\end{aligned} \tag{25}$$

Since $G(z)$ is included in equation (25), it is difficult to achieve this condition as it is. In the conventional VRFT designs (Campi et al., 2002; Sato et al., 2021b), $\boldsymbol{\Gamma}(z,\boldsymbol{\vartheta})$ in the denominator polynomial of equation (22) is replaced with $\boldsymbol{\Gamma}^*(z)$, and $\epsilon_0(z,\boldsymbol{\vartheta})$ is changed as:

$$\begin{aligned}&\epsilon_0'(z,\boldsymbol{\vartheta})\\&= F_W(z)\frac{\boldsymbol{G}(z)(\boldsymbol{\Gamma}^*(z)-\boldsymbol{\Gamma}(z,\boldsymbol{\vartheta}))}{(1+\boldsymbol{G}(z)\boldsymbol{\Gamma}^*(z))(1+\boldsymbol{G}(z)\boldsymbol{\Gamma}^*(z))}.\end{aligned}\tag{26}$$

Therefore, equation (26) equals to equation (24) when $\boldsymbol{F_L}(z)$ is designed as follows:

$$\begin{aligned}&\boldsymbol{F_L}(z)\boldsymbol{\upsilon}_0(z)\\&= F_W(z)\frac{1}{(1+\boldsymbol{G}(z)\boldsymbol{\Gamma}^*(z))}\frac{\boldsymbol{G}(z)\boldsymbol{\Gamma}^*(z)}{(1+\boldsymbol{G}(z)\boldsymbol{\Gamma}^*(z))}\\&= F_W(z)(1-\Omega(z))\Omega(z).\end{aligned}\tag{27}$$

Applying $\boldsymbol{\Upsilon}_0^{-1}(z)$ to the above equation yields equation (16). □

Therefore, instead of $J_0(\boldsymbol{\vartheta})$, the controller parameters are determined based on $J(\boldsymbol{\vartheta})$:

Theorem 1: The optimal controller parameter that minimises equation (6) is obtained from input/output data as follows:

$$\boldsymbol{\vartheta} = Y^{-1}X \tag{28}$$

$$Y = \sum_{k=0}^{N-1}\boldsymbol{\psi}_I(k)\boldsymbol{\psi}_I(k)^\top$$

$$X = \sum_{k=0}^{N-1}\boldsymbol{\psi}_I(k)\upsilon_I(k), \tag{29}$$

where $\upsilon_I(k)$ is the impulse response of $F_W(z)(1-\Omega(z))\Omega(z)$, and

$$\upsilon_I(k) = \mathcal{Z}^{-1}[F_W(z)(1-\Omega(z))\Omega(z)] \tag{30}$$

$$\boldsymbol{\psi}_I(k) = F_W(z)(1-\Omega(z))^2\boldsymbol{\Upsilon}_0^{-1}(z)\boldsymbol{D}(z)[\psi_0(k)]. \tag{31}$$

Proof: Using equation (16), equation (13) is rewritten as follows:

$$\begin{aligned}\epsilon(z,\boldsymbol{\vartheta}) &= F_W(z)(1-\Omega(z))\Omega(z)\\&\quad - F_W(z)(1-\Omega(z))^2\boldsymbol{\Upsilon}_0^{-1}(z)\boldsymbol{\Gamma}(z,\boldsymbol{\vartheta})\psi_0(z).\end{aligned}\tag{32}$$

Equation (32) is described in the time domain as follows:

$$\epsilon(k,\boldsymbol{\vartheta}) = \upsilon_I(k) - \boldsymbol{\psi}_I(k)^\top\boldsymbol{\vartheta}. \tag{33}$$

As a result, using the least-squares method, equation (28) is obtained. □

4 Numerical examples

As a controlled process, consider the next transfer function:

$$G(s) = \frac{100}{s^2+16s+100}. \tag{34}$$

In this simulation, the sampling period of a process output is T_s = 0.1 s, and the holding period of a process input is $T_h = T_s/m$.

Therefore, depending on the value of m, the controlled process is represented as a single-rate system or a dual-rate system, where when m = 1, it is single-rate control; when $m \neq 1$, it is dual-rate control. In order to compare the single-rate and simple dual-rate systems, the process is controlled with m set to 1 and 2, respectively.

The single-rate or dual-rate systems are controlled using the proportional-integral-derivative (PID) control method where the controller structure and parameters are given as follows:

$$\begin{aligned}&\boldsymbol{D}(z) = \boldsymbol{d}(z)^\top \otimes I_m\\&\boldsymbol{d}(z) = [d_1(z)\ d_2(z)\ d_3(z)]^\top\\&d_1(z) = 1, d_2(z) = \frac{1}{1-z^{-1}}, d_3(z) = 1-z^{-1}\\&\boldsymbol{\vartheta} = \begin{cases}\boldsymbol{\vartheta}_1 & \text{(single-rate)}\\ \left[\boldsymbol{\vartheta}_1^\top\ \boldsymbol{\vartheta}_2^\top\right]^\top & \text{(dual-rate)}\end{cases}\\&\boldsymbol{\vartheta}_j = [K_{Pj}\ K_{Ij}\ K_{Dj}]^\top.\end{aligned}\tag{35}$$

It is assumed that the process is controlled stably using an existing single-rate control law with the initial controller parameters as shown in Table 1(a), where the parameters are determined by trial and error, and S-R and D-R denote the single-rate and dual-rate systems, respectively. Figure 3 shows the control result obtained using the initial controller parameters for reference input 1. In Figure 3(a), the reference model output is also plotted, where

$$\Omega(s) = \frac{1}{0.3s+1}. \tag{36}$$

As shown in Figure 3(a), the extremely slow response is obtained since the initial controller parameters are chosen to be conservative. Therefore, the initial controller parameters is not sufficient to track the reference model output, although the process is controlled stably. Figure 3(c) confirms the macing error in the frequency domain.

Table 1 Controller parameters for equation (34)

(a) initial parameters				
		K_{Pi}	K_{Ii}	K_{Di}
S-R	i = 1	0.01	0.01	0.01
(b) tuned in the frequency domain				
		K_{Pj}	K_{Ij}	K_{Dj}
S-R	j = 1	0.2167	2.852	0.0345
D-R	j = 1	0.2191	2.838	0.0343
	j = 2	0.2187	2.837	0.0343
(c) tuned in the time domain				
		K_{Pj}	K_{Ij}	K_{Dj}
S-R	j = 1	0.0744	2.863	0.0055
D-R	j = 1	0.0788	2.834	0.0052
	j = 2	0.0788	2.834	0.0052

Figure 3 Control result of equation (34) using the initial controller, (a) output (b) input (c) gain (see online version for colours)

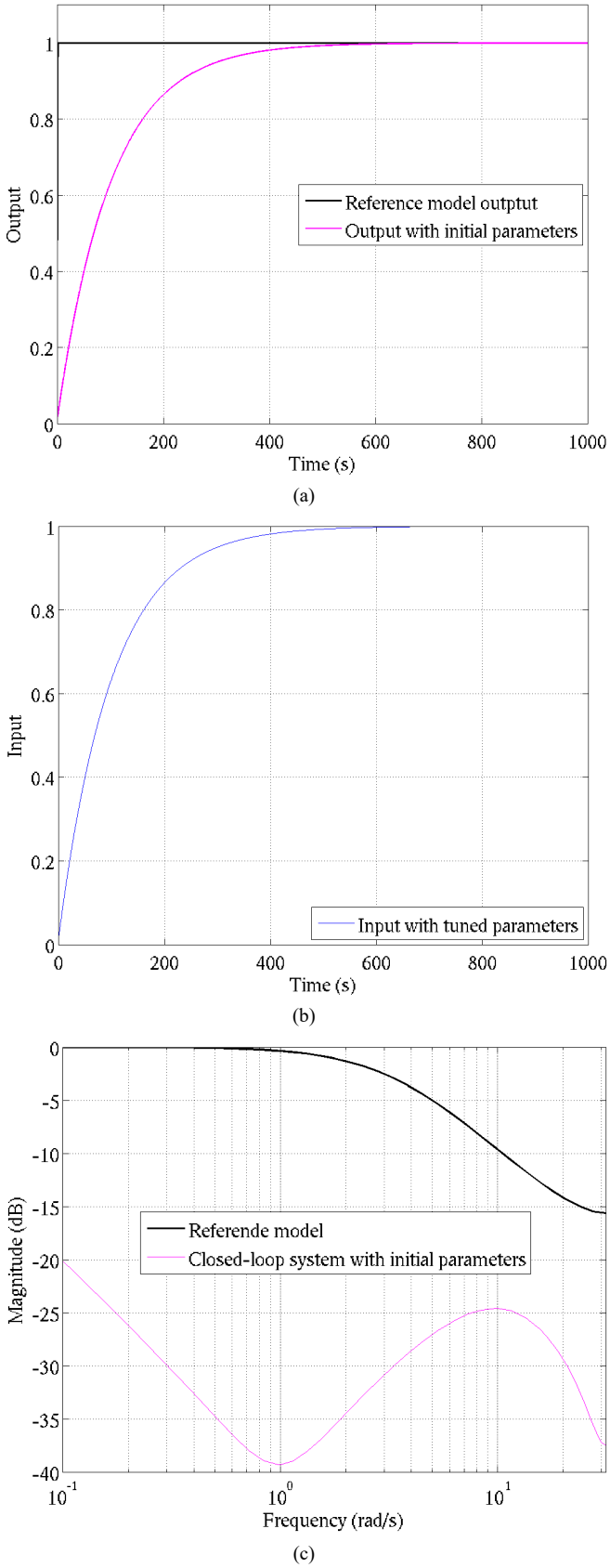

Figure 4 Control result of equation (34) using the frequency-domain designed S-R controller, (a) output (b) input (c) gain (see online version for colours)

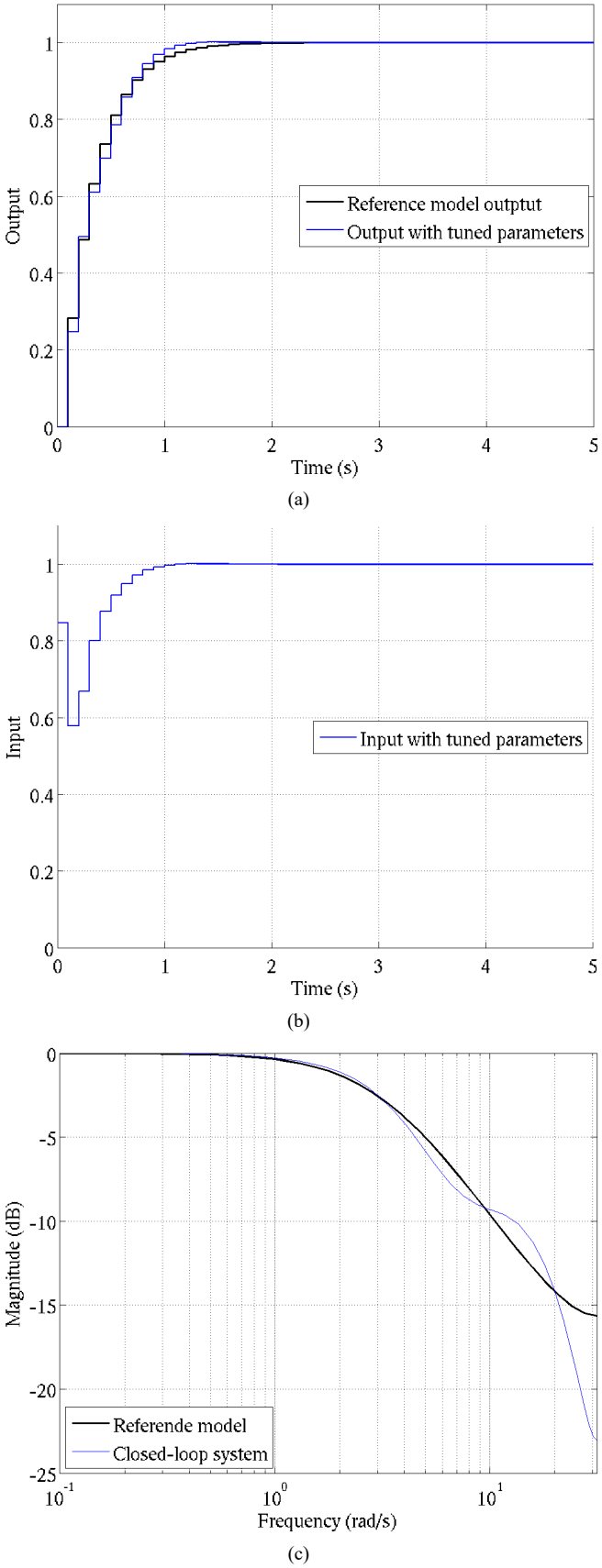

Figure 5 Control result of equation (34) using the frequency-domain designed D-R controller, (a) output (b) input (c) gain (see online version for colours)

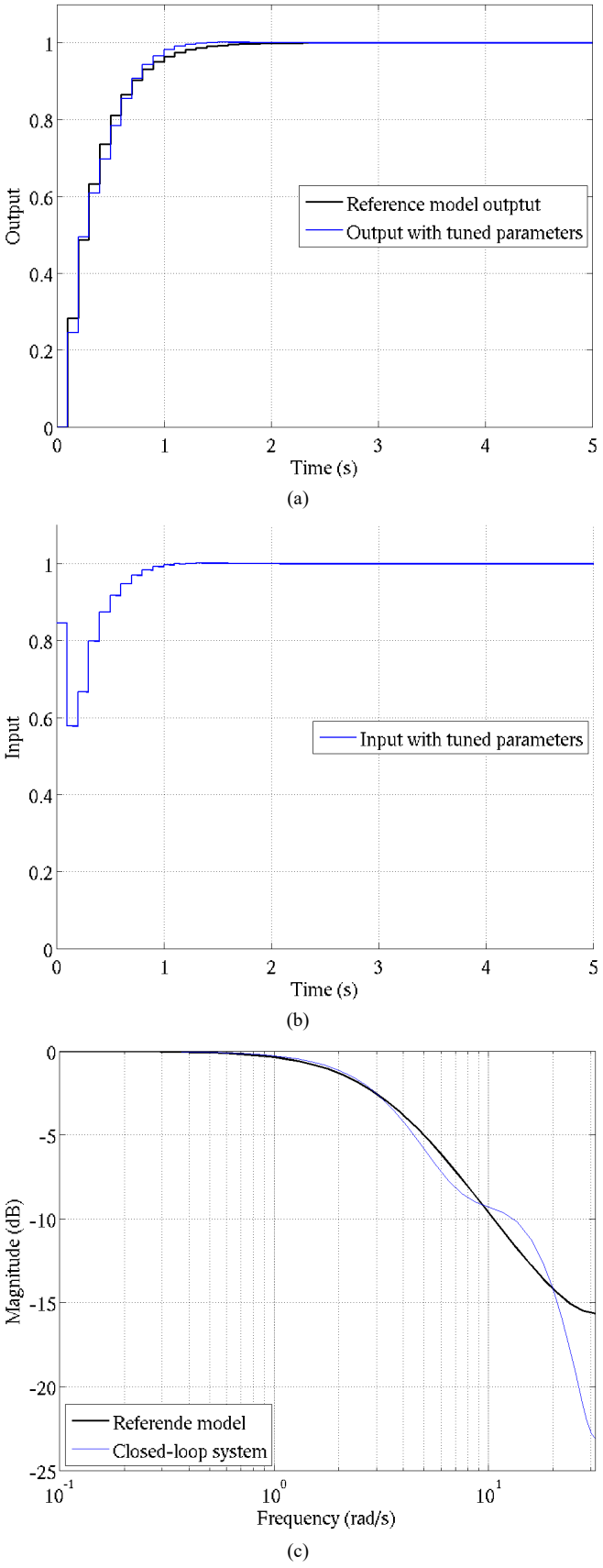

Figure 6 Control result of equation (34) using the frequency-domain designed D-R controller, (a) output (b) input (c) gain (see online version for colours)

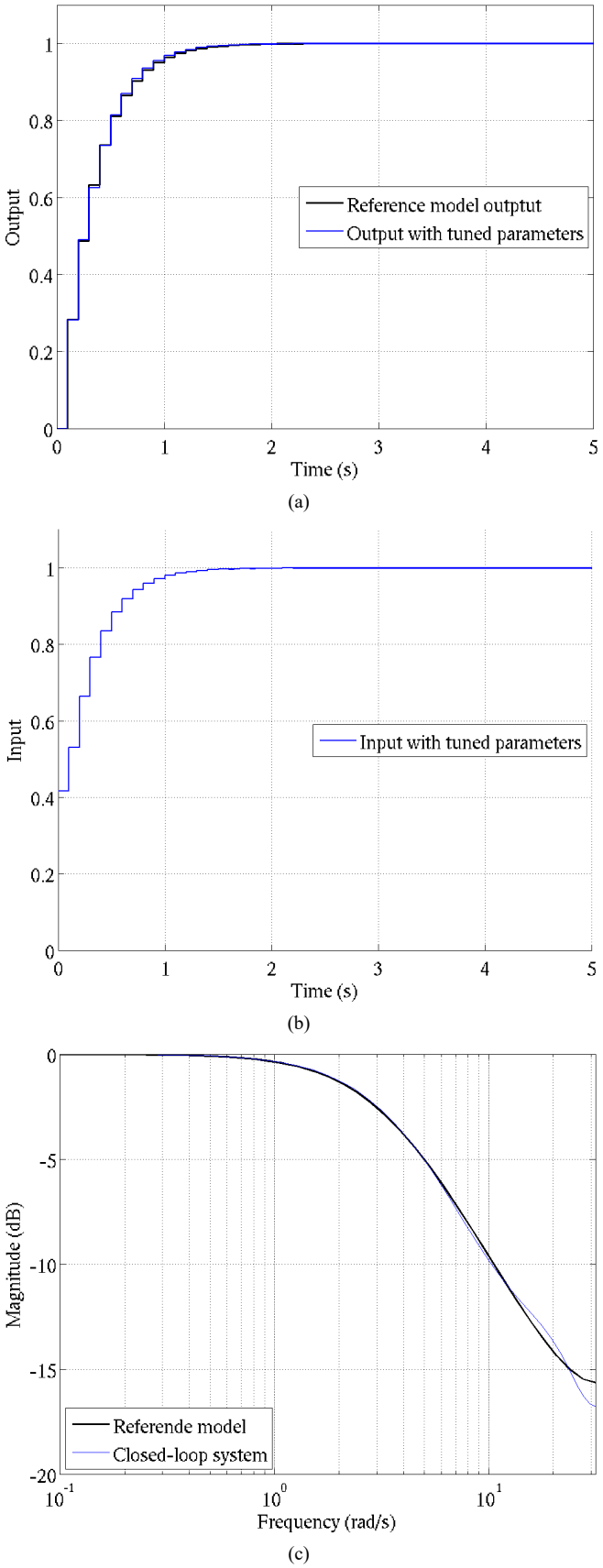

Figure 7 Control result of equation (34) using the time-domain designed D-R controller, (a) output (b) input (c) gain (see online version for colours)

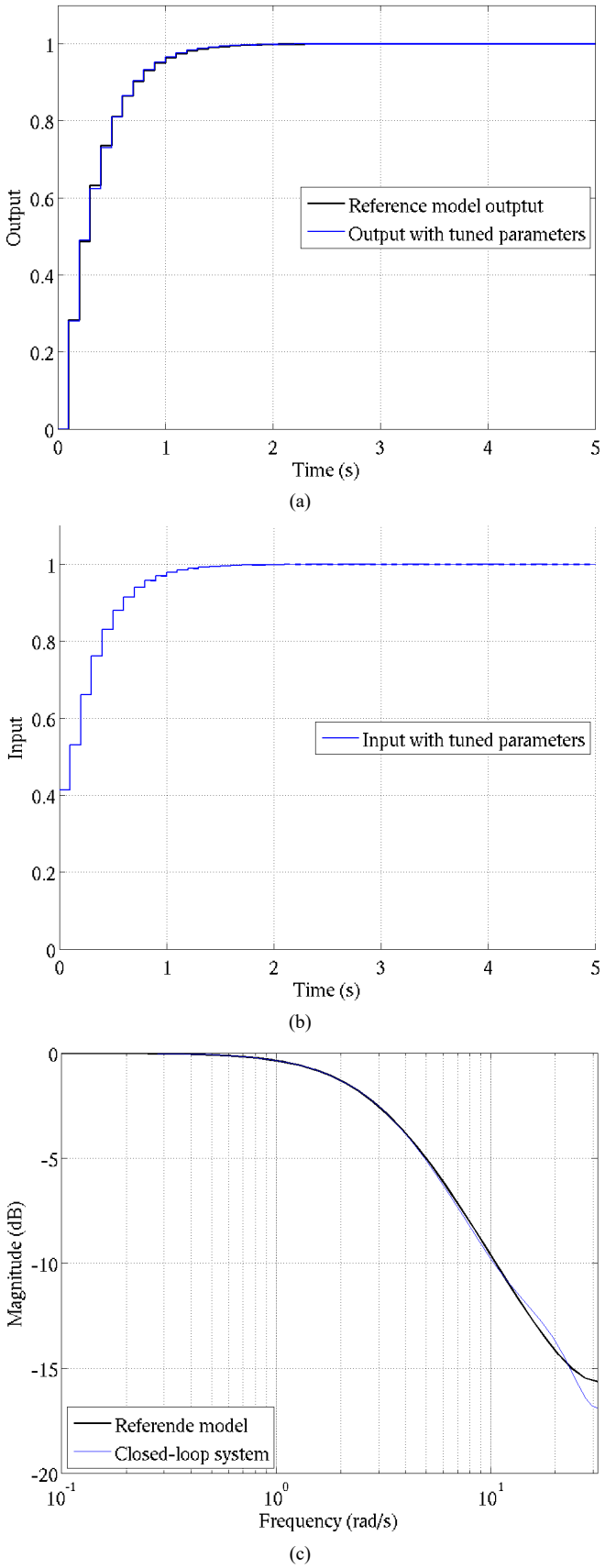

Figure 8 Control result of equation (38) using the initial controller, (a) output (b) input (c) gain (see online version for colours)

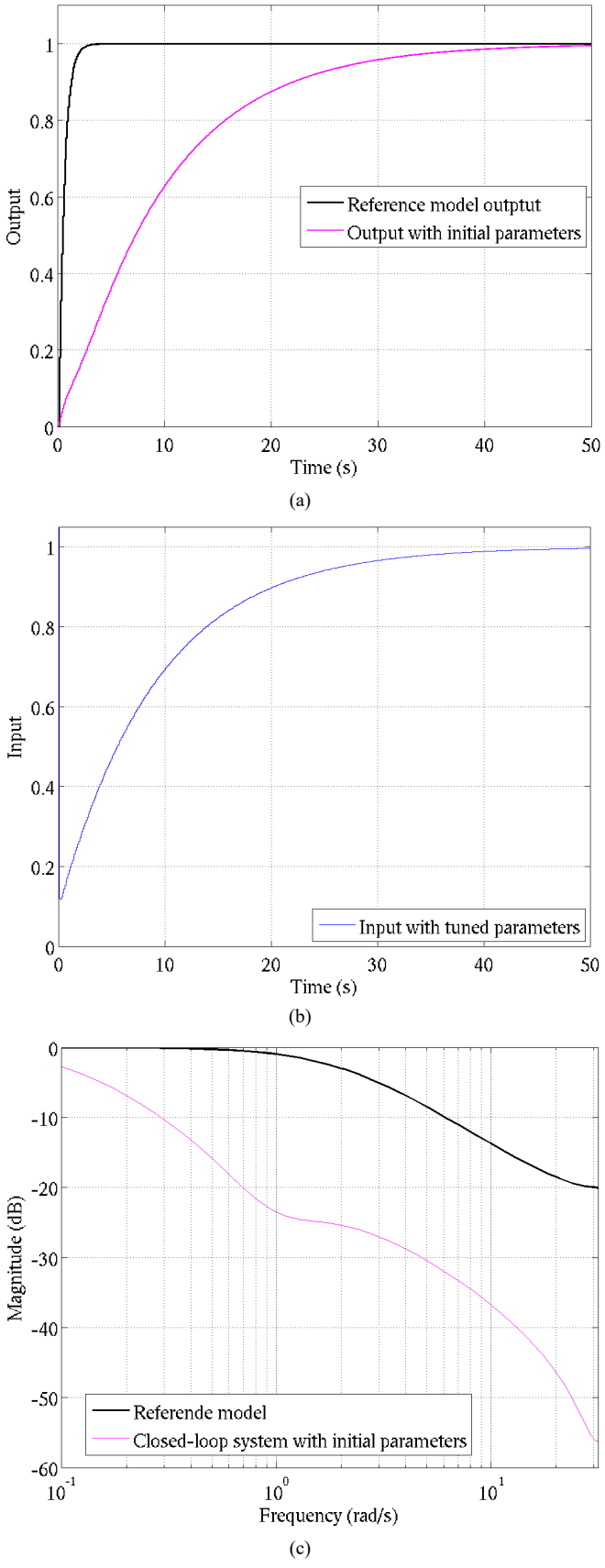

Figure 9 Control result of equation (38) using the frequency-domain designed D-R controller, (a) output (b) input (c) gain (see online version for colours)

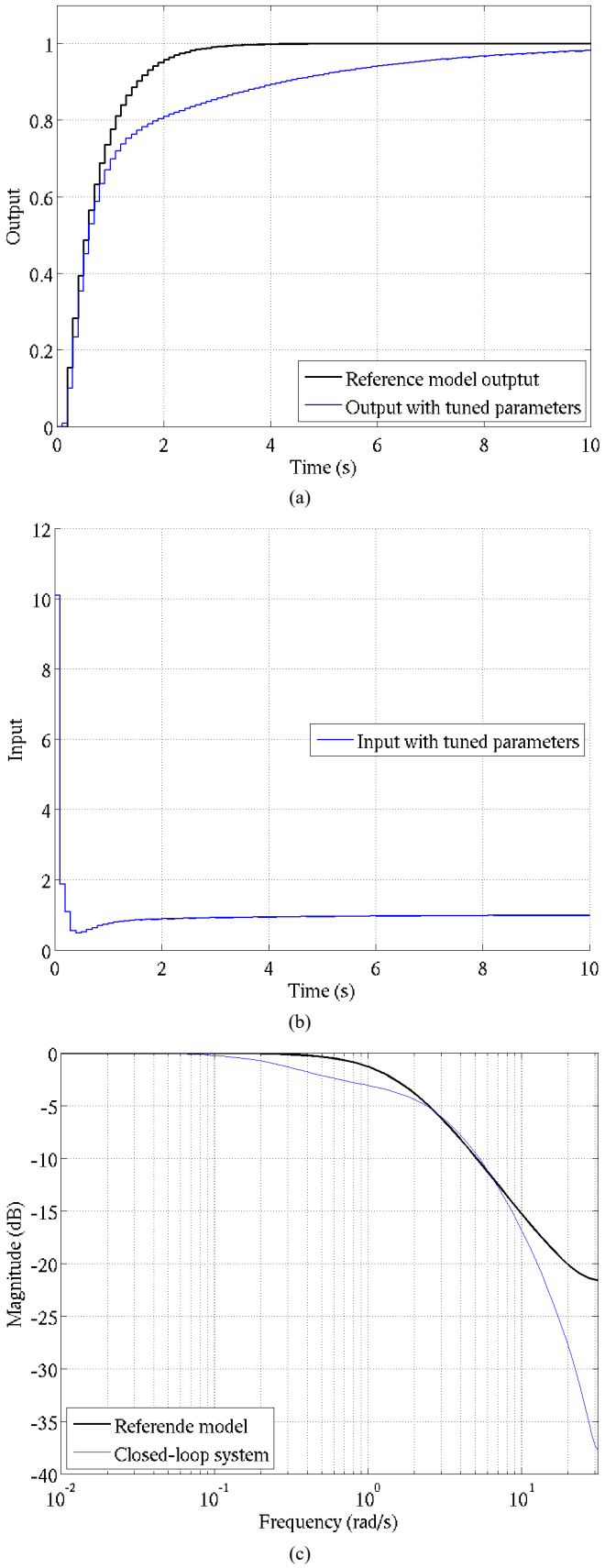

Figure 10 Control result of equation (38) using the time-domain designed D-R controller, (a) output (b) input (c) gain (see online version for colours)

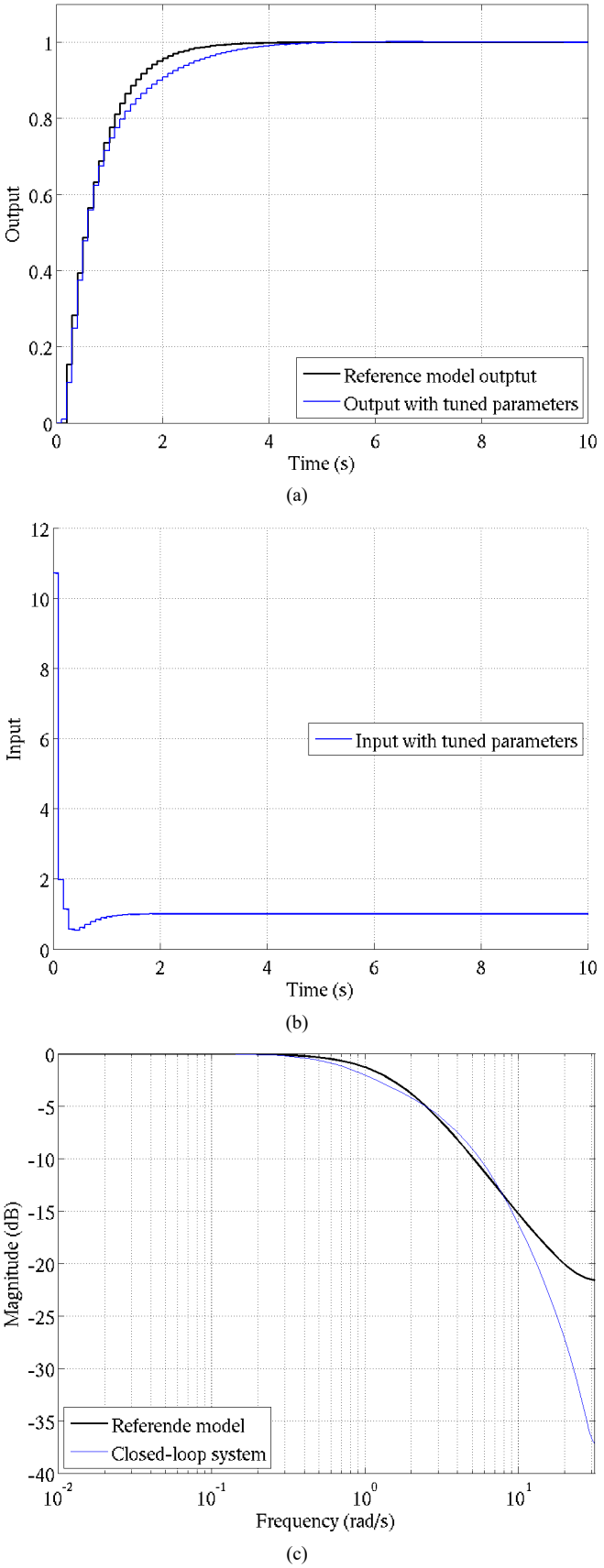

To match the controlled process output to the reference model output, the controller parameters are tuned using the collected data ($N = 500$).

The controller parameters designed in the frequency domain using the conventional methods (Campi et al., 2002; Sato et al., 2021b) are summarised in Table 1(b), where the single-rate and dual-rate PID parameters are tuned based on the same single-rate control data. The controlled results using the tuned single-rate and dual-rate controller parameters are shown in Figures 4 and 5, respectively. Both the single-rate and dual-rate output responses converge to the reference input in the steady state, while both the output responses overshoot slightly.

Based on the same initial control data, the controller parameters are designed in the time domain using the conventional single-rate system and the proposed dual-rate system, respectively, and the obtained parameters are shown in Table 1(c). Comparing the parameters designed in the frequency domain and the time domain, the proportional gains are larger in the time domain than in the frequency domain. Conversely, the integral gains are smaller in the time domain than in the frequency domain. Furthermore, in the dual-rate system design, the PD gains designed in the frequency domain are different, while the PD parameters designed in the time domain are the same values, respectively. The control results using the controller parameters designed in the time domain are shown in Figures 6 and 7. The output responses obtained using the controllers designed in the time domain have a smaller overshoot than those obtained using the controllers designed in the frequency domain.

The obtained control results are evaluated using the following performance function:

$$J_{eval} = \frac{1}{50}\sum_{k=0}^{49}(\psi_\Omega(k) - \psi(k))^2$$
$$\psi_\Omega(z) = \Omega(z)\psi_r(z). \tag{37}$$

The evaluated values are summarised in Table 2. The index values of the time-domain designs are superior to those of the frequency-domain designs, and the index values of the dual-rate designs are also superior to those of the single-rate designs. The above demonstrates the usefulness of the proposed dual-rate time-domain design method.

Table 2 Performance index evaluation for equation (34)

Domain	*Update rate*	J_{eval}
Frequency	S-R (Campi et al., 2002)	1.207×10^{-4}
	D-R (Sato et al., 2021b)	1.205×10^{-4}
Time	S-R (Matsui et al., 2017)	4.486×10^{-6}
	D-R (proposed)	3.177×10^{-6}

Since the frequency- and time-domain design methods have been compared, SR and DR controllers designed with time-domain FIR filter are then compared. The transfer function of a controlled process is given as follows:

$$G(s) = \frac{40^4}{(s^2+64s+160)^2}\frac{1}{(0.8s+1)^2}e^{-0.1s}. \tag{38}$$

The sampling period is 0.1, and the holding periods of S-R and D-R are 0.1 and 0.05, respectively. The gains shown in Table 1(a) are used as initial controller parameters, and the control result is shown in Figure 8. Table 3 shows the tuned controller parameters based on the controlled result as shown in Figure 8. The control results for S-R and D-R controllers using the tuned parameters are shown in Figures 9 and 10, respectively. These results show that the process output by D-R method has a faster rise time and converges to the reference input faster than that by S-R method. In addition, the performance of D-R method in tracking the reference model is better than that of S-R method. Table 4 also shows that the control performance of D-R method is superior to that of S-R method.

Table 3 Tuned in the time domain for equation (38)

		K_{Pj}	K_{Ij}	K_{Dj}
S-R	$j = 1$	1.832	0.6504	0.8200
D-R	$j = 1$	1.843	1.154	0.8755
	$j = 2$	1.843	1.154	0.8755

Table 4 Performance index evaluation for equation (38)

Domain	*Update rate*	J_{eval}
Time	S-R (Matsui et al., 2017)	7.193×10^{-3}
	D-R (proposed)	4.419×10^{-4}

5 Conclusions

In this study, a data-driven design method for dual-rate systems in which the sampling period of the process output is longer than the retention period of the process input is proposed. In the conventional data-driven design method using VRFT for such dual-rate systems, a pr-filter is designed in the frequency domain to convert the data-driven objective function into a model-based objective function. In the proposed method, the pre-filter is designed in the time domain using FIR filter. Numerical examples compare not only single-rate and dual-rate design methods, but also time-domain and frequency-domain design methods. The numerical results show that the proposed time-domain dual-rate design method outperforms both the frequency-domain dual-rate method and the time-domain single-rate method.

Acknowledgements

This study was supported by JSPS KAKENHI Grant Number 22K04158 and Urban Innovation Kobe A22304.

References

Bertsimas, D., Gupta, V. and Kallus, N. (2018) 'Data-driven robust optimization', *Mathematical Programming*, Vol. 167, pp.235–292.

Breschi, V. and Formentin, S. (2021) 'Proper closed-loop specifications for data-driven model-reference control', *IFAC-PapersOnLine, 24th International Symposium on Mathematical Theory of Networks and Systems MTNS 2020*, Vol. 54, No. 9, pp.46–51.

Breschi, V., Persis, C.D., Formentin, S. and Tesi, P. (2021) 'Direct data-driven model-reference control with Lyapunov stability guarantees', in *2021 60th IEEE Conference on Decision and Control (CDC)*, pp.1456–1461.

Bruyne, F. (2003) 'Iterative feedback tuning for internal model controllers', *Control Engineering Practice*, Vol. 11, No. 9, pp.1043–1048.

Campi, M., Lecchini, A. and Savaresi, S. (2002) 'Virtual reference feedback tuning (VRFT): a direct method for the design of feedback controllers', *Automatica*, Vol. 38, No. 8, pp.1337–1346.

Chen, T. and Francis, B. (1995) *Optimal Sampled-Data Control Systems*, Springer-Verlag, London, UK.

Fukuyama, M. (2018) 'Society 5.0: Aiming for a new human-centered society', *Japan Spotlight*, pp.47–50.

Gonçalves da Silva, G.R., Campestrini, L. and Bazanella, A.S. (2016) 'Multivariable VRFT: an approach for systems with non-minimum phase transmission zeros', in *2016 IEEE Conference on Control Applications (CCA)*, pp.1324–1329.

Hjalmarsson, H., Gevers, M., Gunnarsson, S. and Lequin, O. (1998) 'Iterative feedback tuning: theory and applications', *IEEE Control Systems*, Vol. 18, No. 4, pp.26–41.

Ito, S., Sato, T., Araki, N. and Konishi, Y. (2018a) 'Data-driven control system design for a multi-input single-output dual-rate system based on input-multiple closed-loop data', *IEEJ Transactions on Electrical and Electronic Engineering*, Vol. 13, No. 4, pp.654–655.

Ito, S., Sato, T., Araki, N. and Konishi, Y. (2018b) 'Two-loop design for a dual-rate cascade system', in *3rd IFAC Conference on Advances in Proportional-Integral-Derivative Control*, Ghent, Belgium, pp.581–585.

Kaneko, O., Wadagaki, Y. and Yamamoto, S. (2012) 'FRIT based PID parameter tuning for linear time delay systems – simultaneous attainment of models and controllers', in *IFAC Conference on Advances in PID Control*, pp.86–91.

Matsui, Y., Ayano, H., Masuda, S. and Nakano, K. (2016) 'Realization of prefilter for virtual reference feedback tuning using closed-loop step response data', *Journal of Robotics and Mechatronics*, Vol. 28, No. 5, pp.707–714.

Matsui, Y., Ayano, H., Masuda, S. and Nakano, K. (2017) 'Realization of FIR prefilter for virtual reference feedback tuning', *IEEJ Trans. on Electronics, Information and Systems*, in Japanese, Vol. 137, No. 7, pp.pp.884–890.

Prag, K., Woolway, M. and Celik, T. (2022) 'Toward data-driven optimal control: a systematic review of the landscape', *IEEE Access*, Vol. 10, pp.32190–32212.

Rojas, J. and Vilanova, R. (2012) 'Data-driven robust PID tuning toolbox', *IFAC Proceedings Volumes*, Vol. 45, No. 3, pp.134–139.

Sato, T., Araki, N. and Konishi, Y. (2013) 'Design of a multirate pd control system for improvement in the steady-state intersample response', *International Journal of Advanced Mechatronic Systems*, Vol. 5, No. 1, pp.12–19.

Sato, T., Kusakabe, T., Himi, K., Araki, N. and Konish, Y. (2021a) 'Ripple-free data-driven dual-rate controller using lifting technique: application to a physical rotation system', *IEEE Transactions on Control Systems Technology*, Vol. 29, No. 3, pp.1332–1339.

Sato, T., Sakai, Y., Kawaguchi, N. and Arrieta, O. (2021b) 'Dual-rate data-driven virtual reference feedback tuning: improvement in fast-tracking performance and ripple-free design', *IEEE Access*, Vol. 9, pp.144426–144437.

Sato, T., Sakai, Y., Kawaguchi, N. and Inoue, A. (2022) 'Data-driven control for multi-rate multi-input/single-output systems', *ISA Transactions*, Vol. 126, pp.254–262.

Yahagi, S. and Kajiwara, I. (2022) 'Non-iterative data-driven tuning of model-free control based on an ultra-local model', *IEEE Access*, Vol. 10, pp.72773–72784.

Yokoyama, R. and Masuda, S. (2016) 'Data-driven PID gain tuning from regulatory control data based on generalized minimum variance evaluation', in *Proc. of The 7th International Symposium on Design, Operation and Control of Chemical Processes (PSE ASIA 2016)*.

Yokoyama, R., Masuda, S. and Kano, M. (2015) 'Data-driven generalized minimum variance regulatory control for model-free PID gain tuining', in *IEEE International Conference on Control Applications (CCA)*, pp.82–87.

Yubai, K., Terada, S. and Hirai, J. (2011) 'Stability test for multivariable NCbT using input/output data', *IEEJ Trans. of EIS*, Vol. 131, No. 4, pp.773–780.

Appendix

Coefficients of FIR filter

From equation (17),

$$\boldsymbol{\Upsilon}_0^{-1}(z)[\boldsymbol{v}_0(k)] = \begin{cases} 1\,(k=0) \\ 0\,(\text{others}) \end{cases}. \tag{39}$$

Therefore, equation (17) in the time domain is described as follows:

$$\boldsymbol{\Upsilon}\boldsymbol{\nu} = \boldsymbol{\delta}, \tag{40}$$

where

$$\boldsymbol{\Upsilon} = \begin{bmatrix} \boldsymbol{v}_0^\top(0) & \mathbf{0}_{1,l} & \mathbf{0}_{1,l} & \dots & \mathbf{0}_{1,l} \\ \boldsymbol{v}_0^\top(1) & \boldsymbol{v}_0^\top(0) & \mathbf{0}_{1,l} & & \mathbf{0}_{1,l} \\ \vdots & \vdots & \ddots & \ddots & \vdots \\ \boldsymbol{v}_0^\top(N_v-2) & \boldsymbol{v}_0^\top(N_v-3) & \dots & \boldsymbol{v}_0^\top(0) & \mathbf{0}_{1,l} \\ \boldsymbol{v}_0^\top(N_v-1) & \boldsymbol{v}_0^\top(N_v-2) & \dots & \boldsymbol{v}_0^\top(1) & \boldsymbol{v}_0^\top(0) \end{bmatrix} \tag{41}$$

$$\boldsymbol{\nu} = [\boldsymbol{\nu}_0^\top \ \boldsymbol{\nu}_1^\top \ \dots \ \boldsymbol{\nu}_{N_v-1}^\top]^\top \tag{42}$$

$$\boldsymbol{\delta} = [1 \ \mathbf{0}_{1,N_v-1}]^\top, \tag{43}$$

where $\mathbf{0}_{i,j}$ is an $i \times j$ zero matrix, $\boldsymbol{\nu} = \boldsymbol{\Upsilon}^{-1}\boldsymbol{\delta}$ is valid under the condition that the first element of $\boldsymbol{v}_0^\top(0)$ is not 0.